

QUASIEXCITONS IN PHOTOLUMINESCENCE OF INCOMPRESSIBLE QUANTUM LIQUIDS

A. WÓJS* and A. GLADYSIEWICZ

*Institute of Physics, Wrocław University of Technology,
Wrocław 50-370, Poland*

**E-mail: arkadiusz.wojs@pwr.wroc.pl*

J. J. QUINN

*Department of Physics, University of Tennessee,
Knoxville, Tennessee 37996, USA*

The problem of a trion (charged exciton) immersed in an incompressible quantum liquid formed by two-dimensional electrons in a high magnetic field is studied theoretically by combining the composite fermion model and exact numerical diagonalization. Laughlin correlation of the trion with the surrounding electrons is shown to lead to the formation of a family of novel many-body excitations called “quasiexcitons” (QXs). The residual charge of the most stable QX can be either zero or the fractional quantum $\pm e/3$, depending on the presence of negative or positive Laughlin quasiparticles in the electron liquid (controlled by the Landau level filling factor ν), but also on the width of the quantum well, Zeeman spin splitting, etc. The prediction of the magnetic-field driven transition from negative to positive QXs is argued to explain the recently observed minute discontinuity in the photoluminescence spectra of sufficiently wide ($w \geq 20$ nm) asymmetric GaAs quantum wells at $\nu = 1/3$. Conversely, the observed discontinuity is hence indirectly linked to the emergence of a fractional charge quantum in the electron liquid.

Keywords: Trion; Laughlin liquid; Photoluminescence; Fractional quantum Hall effect.

1. Introduction

High magnetic field B applied perpendicularly to a two-dimensional electron gas (2DEG) leads to the quantization of single-particle energy spectrum into the discrete and macroscopically degenerate Landau levels (LLs). At sufficiently large B , corresponding to the cyclotron energy $\hbar\omega_c \propto B$ being much higher than the Coulomb energy scale $e^2/\lambda \propto B^{1/2}$ (where $\lambda = \sqrt{\hbar c/eB}$ is the magnetic length), the low-energy many-body dynamics is completely determined by the electron–electron interaction within an isolated, partially filled LL. Thus, the 2DEG at high B is a unique setting for studying the nonperturbative many-body interaction phenomena, such as the fractional quantum Hall effect,¹ the emergence of incompressible quantum liquids,² or the formation of topological “skyrmion” excitations.³

Photoluminescence (PL) spectroscopy has been used extensively to study the interacting 2D carriers for at least two decades.^{4–8} In a PL experiment, additional

electron–hole (e – h) pairs are introduced into the system through the absorption of photons, and the response of the surrounding carriers makes the recombination spectrum sensitive to the many-electron dynamics. When electrons fill only a small fraction ν of the lowest LL, the PL spectrum is determined by the recombination of bound three-body complexes called trions or charged excitons.^{9,10} A (negative) trion forms from an exciton ($X = e + h$) by capturing another electron ($X^- = X + e$). It is analogous to a Hydrogen ion H^- , although with quite different energy and length scales, making the X^- much more susceptible to the external perturbations. The trion energy spectrum depends on B and also on the composition, width w , and doping of the quantum well.¹¹ In general, several bound trion states occur, distinguished by the pair-electron spin (singlet vs. triplet), total angular momentum, and optical lifetime (dark vs. bright). The binding energies are typically 1–2 meV.

The situation is more complicated at higher LL fillings $\nu = 2\pi n\lambda^2$ (where n is the 2D electron concentration). In this situation, the trions interact with the surrounding electrons and can no longer be regarded as isolated, well-defined three-body quasiparticles. In fact, it is precisely the coupling of trions with the 2DEG which allows (in principle) the many-electron dynamics to be indirectly probed by the trion recombination in a PL experiment.

The history of experiments showing features in the PL spectrum coincident with electron incompressibility goes back a long time.^{4,5,7,8,10} However, no earlier realistic theory has (in our opinion) explained what happens to a trion when it is immersed into a 2DEG. Several ideas were proposed, including decoupling of neutral excitons^{12,13} or formation of “anyon excitons”.^{14,15} Yet the simple models are not applicable to the experimental situation in which the anomalies in PL are observed, and not even qualitative agreement has been found.

In this note, we use a composite fermion (CF) model and the idea of magnetic flux attachment to explain how a trion correlates with the 2DEG to become a new, fractionally charged excitation called a quasiexciton (QX). In short, the QX is another kind of a CF, only made of a trion instead of an electron. The emergence of QXs under reasonable experimental conditions is predicted by the realistic numerical calculations carried out for doped GaAs 10–20 nm wells, with electron concentration $n = 2 \cdot 10^{11} \text{ cm}^{-2}$ for which the Laughlin $\nu = 1/3$ state² occurs at a high yet accessible $B = 25 \text{ T}$. The family of neutral, positive, and negative QX states is identified in the $Ne + h$ energy spectra ($N \leq 10$) in Haldane’s spherical geometry. The QX binding energies and recombination rates depend on the involved trion state. As a result, the PL spectrum at $\nu \approx 1/3$ depends sensitively on the well width w . We predict no anomaly for $w = 10 \text{ nm}$, a small (0.25–0.5 meV) splitting or discontinuity for $w = 20 \text{ nm}$, and a different, larger splitting for $w \geq 40 \text{ nm}$.

2. Numerics on a Haldane Sphere

In the numerical calculations we use spherical geometry,¹⁶ with the magnetic field normal to the surface (i.e., radial) produced by a Dirac monopole of strength $2Q$

defined in the units of flux quantum, $2Q (hc/e) = 4\pi R^2 B$. The radius of the sphere R and the magnetic length λ are connected by $Q\lambda^2 = R^2$, which also relates $2Q$ with the surface curvature (in the units of λ^{-1}). The LLs on a sphere have the form of degenerate angular momentum shells with $l \geq Q$. To make calculations realistic, we take advantage of a 2D rotational symmetry of spheres with finite LL degeneracy, but use cyclotron energies and interaction matrix elements of an actual experimental system. The finite-size and surface-curvature errors are minimized by extrapolation of the results to $\lambda/R \rightarrow 0$. More details were given elsewhere.^{11,17}

3. Isolated Trion

The X^- binding energies Δ in GaAs wells were obtained¹⁷ from diagonalization of the $e + h$ and $2e + h$ hamiltonians at $2Q \leq 25$. For $e + h$, the lowest-energy band is the exciton energy dispersion, energy E_X as a function of wave vector k . In closed geometry, k must be quantized. On a sphere, it is represented by the total angular momentum related to k through $L = kR$. In particular, the $k = 0$ excitonic ground state appears at $L = 0$. For $2e + h$, the spectrum splits into the bound and unbound states. The bound states are those with the positive binding energy, $\Delta = E_X - E_{X^-}$ (where the electron energy at the lowest LL is taken as zero). Due to nonzero electric charge, bound trion states in a magnetic field are labeled by the relative angular momentum M rather than by a wave vector. On a sphere, different values of M correspond to different total angular momenta L , according to the following relation $M = Q - L$. Based on L (i.e., on M), the trions are either “bright” or “dark”, meaning that they either can or cannot recombine radiatively ($X^- \rightarrow e + \gamma$ where γ is a photon) in the absence of an additional symmetry breaking collision. The criterion for a “bright” trion state is $L = Q$ (i.e., $M = 0$). Another good trion quantum number is the pair electron spin $S = 0$ or 1 .

In the realistic calculation, five LLs and two quantum well subbands for both e and h were included, and the quasi-2D interaction matrix elements were integrated taking the actual e and h subband wave functions $\chi(z)$ in the normal direction. The dependence of $\chi_e(z)$ and $\chi_h(z)$ on well width w and electron concentration n was calculated self-consistently,¹⁸ assuming doping on one side of the well.

Some results are shown in Fig. 1. Despite significant separation of e and h layers, the X^- occurs even in a fairly wide ($w = 20$ nm) and fairly strongly (asymmetrically) doped ($n = 2 \cdot 10^{11}$ cm⁻²) quantum well. Remarkably, neither the lowest-subband, lowest-LL, or symmetric-well approximations are satisfactory for this well. For the purpose of the following discussion, let us observe that, assuming $n = 2 \cdot 10^{11}$ cm⁻² and $B = 25$ T, the ground state in a narrow, $w = 10$ nm well is the “bright singlet” X_s^- , while for a wider, $w = 20$ nm well it is the “dark triplet” X_t^- (note that the plotted Δ excludes the Zeeman term that weakens binding of the singlet state). The other trion in Fig. 1 is the marginally bound “bright triplet” X_{tb}^- .

Remarkably, the trion spectrum for $w = 20$ nm resembles that of an “ideal” system ($w = 0, B = \infty$) more than the spectrum for $w = 10$ nm. The ideal system

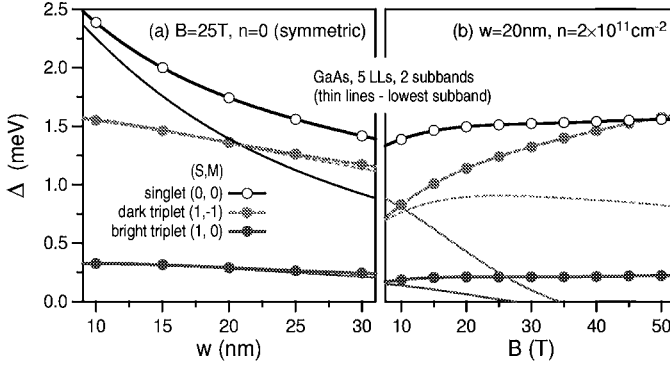


Fig. 1. (a) The X^- Coulomb binding energy Δ as a function of width w of a symmetric (or undoped) GaAs quantum well, at the magnetic field $B = 25$ T, calculated including five Landau levels and one (thin lines) or two (thick lines with symbols) well subbands for both electrons and the hole. Different trion states are labeled by spin S and relative angular momentum M . (b) Δ as a function of B , in a $w = 20$ nm well doped on one side to electron concentration $n = 2 \cdot 10^{11}$ cm $^{-2}$.

obeys the “hidden” (particle–hole) symmetry,¹² which implies the occurrence of “multiplicative” states,¹³ only one bound trion state (X_t^-),¹⁹ and simple selection rules for e – h recombination. In narrow wells, the hidden symmetry is broken by a stronger confinement of the hole (in all three dimensions) causing imbalance between the e – h and e – e interactions and, for example, binding of the X_s^- . In wider wells, the e – h separation reduces the interaction imbalance and favors the X_t^- .

4. Trion in 2DEG

When the X^- is immersed in a 2DEG, its effective, residual electric charge Q (counted from the uniform electron density n) depends on the exact form of e – X^- correlations. This is shown schematically in Fig. 2(a). In the lowest LL, the similar (i.e., strongly repulsive at short range) e – e and e – X^- Haldane interaction pseudopotentials²⁰ cause similar (Laughlin) e – e and e – X^- correlations.¹¹ They are described in a generalized²¹ composite fermion (CF) picture²² involving attachment of $2p$ flux quanta to each e and X^- .

At a Laughlin–Jain (LJ) series of $\nu_{LJ} = s/(2ps + 1)$, electrons converted to CF_e ’s fill the lowest s LLs in effective magnetic field $B^* = B - 2pn(\hbar c/e) = B/(2ps + 1)$. At ν larger or smaller than ν_{LJ} , the LJ quasiparticles (QPs) occur in form of quasielectrons (QEs) in the $(s + 1)^{st}$ or quasiholes (QHs) in the s^{th} CF_e -LL, each carrying an effective charge $\varepsilon = \pm e/(2ps + 1)$. Similarly, an X^- in a LJ liquid is converted to a CF_{X^-} with the reduced charge $Q = -\varepsilon$. In contrast to the CF_e ’s, there is only few CF_{X^-} ’s so they all fall into the lowest, nearly empty CF_{X^-} -LL. Thus, the strongly correlated 2DEG with an immersed trion is mapped onto the system of a smaller number of weakly correlated QPs and CF_{X^-} ’s. The number (effective filling factor) and type of the QPs (QEs, QHs, or both) depends in a

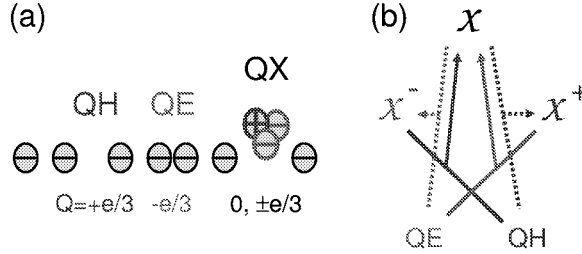


Fig. 2. (a) Partial screening of a trion immersed in a 2D electron liquid with Laughlin correlations, leading to the formation of a family of neutral and fractionally charged quasiexciton (QX) states. (b) Transitions between different QXs ($\mathcal{X}^- \leftrightarrow \mathcal{X} \leftrightarrow \mathcal{X}^+$) in the presence of free QEs or QHs.

nontrivial manner on ν and also to some extent on temperature. On the other hand, the number of $\text{CF}_{\mathcal{X}^-}$'s is controlled by the power density of the optical excitation. It can be typically assumed negligible, thus allowing for considering an isolated $\text{CF}_{\mathcal{X}^-}$ interacting with a varied type and concentration of QPs.

This result is independent of the particular \mathcal{X}^- state or the filling factor, as long as the correlations are described by the CF model. The fact that $\mathcal{Q} \neq 0$ means that the electrons surround the \mathcal{X}^- more closely than they surround each other. In other words, because of the severe restriction of the electron motion to the lowest LL (caused by the presence of a strong magnetic field), the LJ liquid cannot screen completely a foreign charge (e.g., an \mathcal{X}^-). Instead, it leaves a residual fractional charge $\mathcal{Q} \neq 0$, equal to the charge of one CF quasiparticle. The nonzero value of \mathcal{Q} can also be linked to the fact that the \mathcal{X}^- is distinguishable from the macroscopic number of the surrounding electrons, reflected in the macroscopic degeneracy of the 2DEG- \mathcal{X}^- ground state (i.e., of the $\text{CF}_{\mathcal{X}^-}$ -LL). Moreover, the same value of \mathcal{Q} results for any distinguishable charge $-e$ immersed in a LJ liquid, if it induces Laughlin correlations around itself.²³

5. Neutral and Charged Quasiexcitons

A trion coupled to a LJ liquid and carrying a reduced charge $\mathcal{Q} = -\varepsilon$ is a many-body excitation. To distinguish it from the isolated three-body state $\mathcal{X}^- = 2e + h$, we call it a charged quasiexciton (QX) and denote by $\mathcal{X}^- \equiv \mathcal{X}^{-\varepsilon}$.

Being negatively charged, an \mathcal{X}^- interacts with the QPs of the LJ liquid, attracting the QHs and repelling the QEs. Indeed, as shown schematically in Fig. 2(b), the problem of a trion coupled to a 2DEG can be reformulated as that of the QXs interacting with the QPs.

At $\nu < \nu_{\text{LJ}}$, there are free QHs in the LJ liquid, making the negative \mathcal{X}^- unstable. By means of direct Coulomb attraction, the \mathcal{X}^- binds a QH to become a neutral $\mathcal{X}^- \text{QH} = \mathcal{X}$, with a binding energy called Δ^0 . The neutral \mathcal{X} may or may not bind an additional QH to form a positively charged $\mathcal{X}^- \text{QH}_2 = \mathcal{X}^+$, with binding energy Δ^+ . Whether it does (i.e., whether $\Delta^+ > 0$) depends on the details

of the \mathcal{X} wave function, that is on the spin of the “parent” trion X^- , which in turn depends on various parameters of the quantum well.

At $\nu > \nu_{LJ}$, there are free QEs in the LJ liquid. This makes the positive \mathcal{X}^+ attract and annihilate a QE: $\mathcal{X}^+ + \text{QE} \rightarrow \mathcal{X}$. Such process releases the energy $\Delta_{LJ} - \Delta^+$ (where $\Delta_{LJ} = \mathcal{E}_{QE} + \mathcal{E}_{QH}$ is the LJ gap). The \mathcal{X} may or may not (again, depending on the “parent” X^- , that is on the specific quantum well parameters) annihilate another QE: $\mathcal{X} + \text{QE} \rightarrow \mathcal{X}^-$, with the energy gain

$$\Delta^- = \Delta_{LJ} - \Delta^0 \quad (1)$$

that can be interpreted as \mathcal{X}^- binding energy.

The neutral \mathcal{X} and charged \mathcal{X}^\pm are the three possible states in which a valence hole can exist in a LJ fluid. If $\Delta^\pm > 0$, then depending on ν , either \mathcal{X}^- or \mathcal{X}^+ is the most strongly bound state. If $\Delta^- \neq \Delta^+$, they will recombine at a different energy and the PL spectrum will be discontinuous at $\nu = \nu_{LJ}$. For long-lived \mathcal{X}^\pm (e.g., made of a dark X_t^-), recombination of the \mathcal{X} is also possible, especially at $\nu \approx \nu_{LJ}$ (within a Hall plateau), when the QP localization impedes the \mathcal{X}^\pm binding.

The QXs resemble normal excitons and trions in n - or p -type systems, with the QPs (QEs and QHs) playing role of conduction electrons and valence holes. Remarkably, the type and concentration of the QPs can be controlled in the same sample by tuning the magnetic field. In particular, the QP gas converts from effectively n - to p -type (from consisting of QEs to QHs) when the magnetic field is increased so that the filling factor passes through $\nu = 1/3$. Another important difference between the normal trions and charged QXs is the fractional charge of the constituent QPs, responsible for the adequately smaller binding energies. Also, the kinetics of QXs ($\mathcal{X} \leftrightarrow \mathcal{X}^\pm$) is more complicated because of the involved QE–QH annihilation.

6. QX Spectra for $w = 20$ nm

The above reasoning based on a CF model has been tested by realistic numerical calculations for the incompressible Laughlin $\nu = 1/3$ quantum liquid. We have calculated the energy and recombination spectra of $N \leq 10$ electrons and one hole assuming concentration $n = 2 \cdot 10^{11} \text{ cm}^{-2}$ for which $\nu = 1/3$ occurs at $B = 25$ T.

For $w = 20$ nm, the most strongly bound trion is the X_t^- . This is apparent from Fig. 1, after the plotted Coulomb binding energy of the singlet trion is decreased compared to the triplet trion by the electron Zeeman term $E_Z = g^* \mu_B B = 0.75$ meV. From the diagonalization of a $2e + h$ hamiltonian we have established that the X_t^- has a high (94%) squared projection onto the subspace of the lowest LL and the lowest subband. This allows one to restrict the $Ne + h$ calculation to this smaller and thus numerically tractable (spin-polarized) subspace. The results for $N = 9$ are shown in Fig. 3, where the energy E is plotted as a function of the total angular momentum L , and the PL oscillator strengths τ^{-1} of radiative states are indicated by the diameter of the open circles.

These spectra can be understood using a CF picture generalized to a two-component fluid²¹ and the addition rules for angular momentum. On a sphere, the

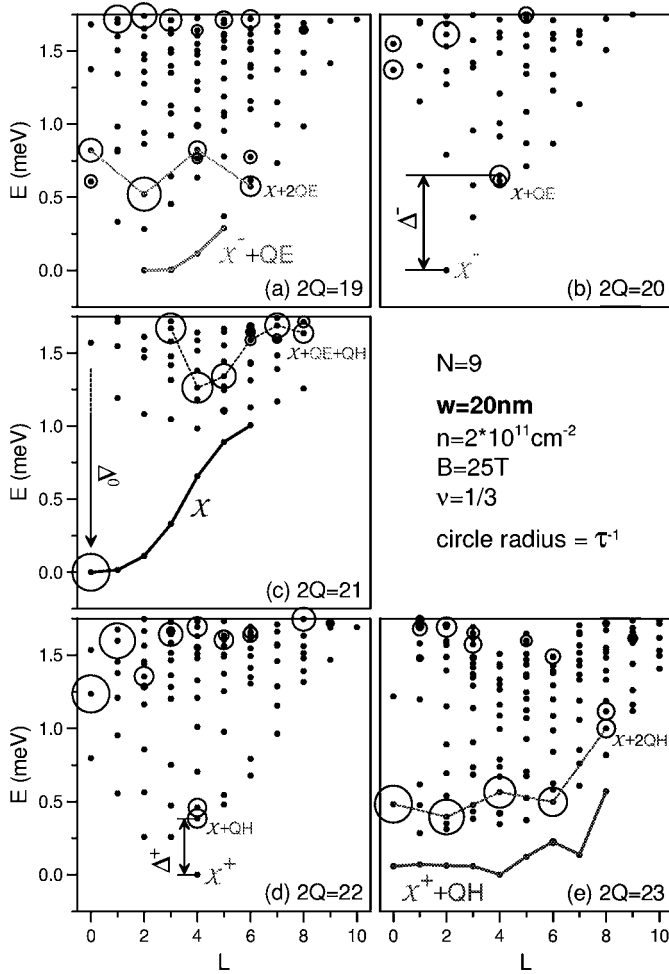


Fig. 3. Excitation spectra (energy E as a function of angular momentum L with the optical oscillator strength indicated by the diameter of the circles) of $9e+h$ systems on a Haldane sphere, at the values of $2Q$ corresponding to up to two QEs or QHs in the Laughlin $\nu = 1/3$ liquid.

CF transformation introduces an effective monopole strength $2Q^* = 2Q - 2(K - 1)$, where $K = N - 1$ is the total number of free charges (electrons and trions). The angular momenta of Laughlin QPs are $l_{\text{QH}} = Q^*$ and $l_{\text{QE}} = Q^* + 1$. And since the X_t^- had $l_{X^-} = Q - 1$, the effective X^- angular momentum is $l_{X^-} = Q^* - 1$ (in the following discussion for $w = 20$ nm we use $X \equiv X_t$).

The X^- is found at $2Q = 20$, as a dark ground state at $L = l_{X^-} = 2$. At $2Q = 22$, there are two QHs in addition to the X^- , and the X^+ bound state is identified at $L = l_{X^+} = |(2l_{\text{QH}} - 1) - l_{X^-}| = 4$.

The bands of interacting X^- -QE and X^+ -QH pairs are marked at $2Q = 19$ and 23 (they terminate at $L < l_{X^\pm} + l_{\text{QP}}$ because of a hard-core reflecting the composite

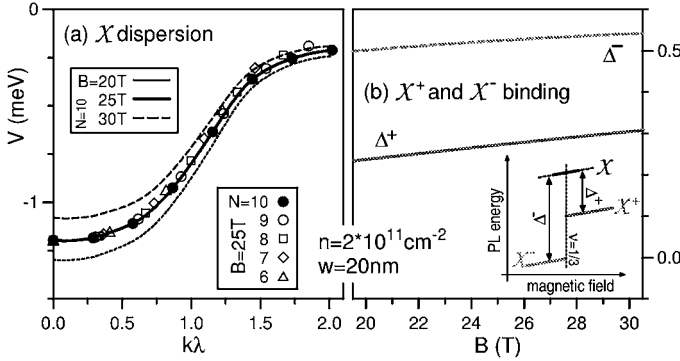


Fig. 4. Dispersion (interaction energy V as a function of wave vector k) of the neutral quasiexciton \mathcal{X} (a) and the binding energies Δ^\pm of charged quasiexcitons \mathcal{X}^\pm (b) in a Laughlin $\nu = 1/3$ liquid. Inset: predicted discontinuous field-dependence of the PL energy. λ is the magnetic length.

nature of the QX and the Pauli exclusion principle for its fermion constituents²¹). The increase of $E(L)$ in these bands confirms \mathcal{X}^- -QE and \mathcal{X}^+ -QH repulsion (on a sphere, larger L corresponds to a smaller average squared separation), with the strength comparable to the known QP-QP interactions.

At $2Q = 21$, there is one \mathcal{X}^- and one QH. The radiative ground state at $L = 0$ is (approximately) a multiplicative state. This means that it contains an X which has $k = 0$ and is decoupled from the Laughlin state of $K = 8$ electrons. It opens a band of \mathcal{X}^- -QH pair states (the sum of l_{QH} and $l_{\mathcal{X}^-}$ giving $L = 1$ to 6).

This can be understood as follows. An isolated, stationary X (with wave vector $k = 0$) has no dipole moment ($d = 0$). When it moves ($k > 0$), Lorentz force acts on its constituents and induces charge separation ($d \propto k$), and the X splits into e and h , each carrying charge $\pm e$. In a LJ liquid, charge quantum is reduced to ε . This has no consequence at $k = 0$, and the \mathcal{X} is equivalent to an X decoupled from the remaining K electrons. But a moving \mathcal{X} acquires dipole moment in a different way than X, by splitting into \mathcal{X}^- and QH, each carrying only one small quantum $\pm\varepsilon$. The continuous dispersion of \mathcal{X} (the \mathcal{X}^- -QH pseudopotential) at $\nu = 1/3$, obtained by the extrapolation of data for $N \leq 10$, is shown in Fig. 4(a). Its energy and length scales are comparable to the dispersion of X rescaled to account for the $e \rightarrow \varepsilon$ charge reduction.

By identifying the multiplicative states (from comparison with the spectra of ideal systems) and knowing that $\mathcal{X} \equiv X$ at $k = 0$, one can estimate the \mathcal{X}^- binding energies Δ^\pm as marked in frames (b) and (d). More accurate values can be obtained from the comparison of energies obtained from different spectra in which there is always only one particular constituent (\mathcal{X}^\pm , \mathcal{X} , or QP) in the Laughlin liquid. These values were further extrapolated to $N \rightarrow \infty$, and the result is plotted in Fig. 4(b) as a function of B . The \mathcal{X} binding energies Δ^0 were obtained in the same way, and the $V(0) \equiv \Delta^0$ equivalence was used to vertically shift dispersion curves in Fig. 4(a).

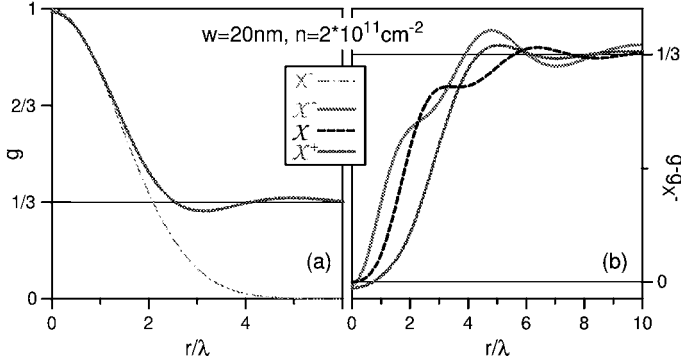


Fig. 5. (a) Comparison of the e - h pair-distribution functions (electron density g normalized so as to converge to the filling factor ν far away from the hole, as a function of the e - h distance r) of the positive quasixciton \mathcal{X}^+ and the bare trion X_t^- . (b) The e - X^- pair-distribution functions calculated as the difference between the $\mathcal{X}/\mathcal{X}^\pm$ and X_t^- curves in (a). λ is the magnetic length.

Reasonable accuracy of our estimates for QX binding energies is confirmed by Eq. (1). Our values (GaAs, $w = 20$ nm, $n = 2 \cdot 10^{11}$ cm $^{-2}$, $\nu = 1/3$, $B = 25$ T) are: $\mathcal{E}_{QH} = 0.73$ meV, $\mathcal{E}_{QE} = 1.05$ meV, $\Delta^0 = 1.20$ meV, $\Delta^- = 0.52$ meV, and $\Delta^+ = 0.27$ meV. The $\Delta^+ \neq \Delta^-$ asymmetry is expected to make emission energy discontinuous at $\nu = 1/3$. PL spectra qualitatively similar to our prediction shown in the inset in Fig. 4(b) were already been observed^{5,8} at $\nu \approx 1/3$.

7. QX Wave Functions for $w = 20$ nm

The QXs are defined through the following sequence of gedanken processes: (i) trion binding: $2e + h \rightarrow X^-$, (ii) charge reduction: $X^- \rightarrow \mathcal{X}^-$, (iii) QH capture: $\mathcal{X}^- \rightarrow \mathcal{X}$ or \mathcal{X}^+ . Hence, the \mathcal{X}^- , \mathcal{X} , and \mathcal{X}^+ states in fact involve the same X^- , only more or less spatially separated from the surrounding electrons.

This is evident in Fig. 5(a) showing the e - h pair-distribution function $g(r)$ of the positive QX, calculated for $N = 10$ and normalized so as to measure electron concentration near the hole in the units of ν . At short range, it is quite similar to $g_{X^-}(r) = \exp(-r^2/4)$ accurately describing an X_t^- . This confirms that the \mathcal{X}^+ is an X^- well separated from the 2DEG. In Fig. 5(b) we plotted $\delta g = g - g_{X^-}$, measuring e - X^- correlations in the QX states. Clearly, $\delta g_{\mathcal{X}^+}$ resembles the e - e pair-distribution function of a Laughlin $\nu = 1/3$ liquid, with shoulders in $\delta g_{\mathcal{X}}$ and $\delta g_{\mathcal{X}^-}$ reflecting additional charge quanta pushed onto the hole in \mathcal{X} and \mathcal{X}^- . Moreover, integration of $[g(r) - 1/3]$ reveals fractional electron charge of $-(4/3)e$, $-e$, and $-(2/3)e$ bound to the hole in the \mathcal{X}^- , \mathcal{X} , and \mathcal{X}^+ states.

8. QX Spectra for $w = 10$ nm

The QX concept can in principle be applied to any incompressible CF state. This might seem to imply complicated, nonmonotonic dependence of Q on B , and the

entire LJ series of discontinuities in PL of a 2DEG, with the energy jumps $\propto \varepsilon^2/\lambda$. However, a discontinuity at each particular ν_{LJ} depends on the (sample-dependent) relation between Δ_{LJ} and Δ^0 , and must be established separately.

The other quantum well we studied had the same n , but a smaller $w = 10$ nm. It is apparent from the trion spectra in Fig. 1 (we have also checked that in narrow wells, such as with $w = 10$ nm, the effect of electron concentration n or doping asymmetry on Δ is negligible) that the lowest (QX) states at $\nu \approx 1/3$ will contain an X_s^- . This singlet trion state involves a spin-flip, and its binding depends critically on the LL mixing (only the X_t^- remains bound in the lowest LL). This complicates calculations and led us to the following approximation.

In the computation of Coulomb matrix elements, the highest Haldane $e-e$ pseudopotential,²⁰ V_0 , was reduced by 10%. We have checked that this only affects interactions within the trion, and induces an (85% accurate) X_s^- ground state *within the lowest LL*. Critically for the purpose of our calculation, it has the correct pair-distribution functions g_{eh} and g_{ee} , which determine the investigated coupling of the trion to the surrounding 2DEG. Hence, the $Ne + h$ spectra calculated with one reversed-spin electron and using the reduced V_0 capture the essential difference between QX dynamics in 20 and 10 nm wells.

Such spectra for $N = 8$ are presented in Fig. 6. From the comparison of PL oscillator strengths τ^{-1} (separate for recombination of a spin- \uparrow or \downarrow electron) we identified the (approximately) multiplicative states with a stationary $\mathcal{X} \equiv \mathcal{X}_s$. An expected difference from Fig. 3 is that since low-energy states involve a (bright) X_s^- , they are all radiative. But surprisingly, charged QXs are now the excited states at $2Q = 17$ and 19 (when calculating L , note that $l_{\mathcal{X}^-} = Q^*$ for X_s^-). The multiplicative states with an \mathcal{X} and two QPs (rather than an \mathcal{X}^- -QE or \mathcal{X}^+ -QH pair) also form the lowest bands at $2Q = 16$ and 20.

The origin of such different behavior in narrow and wide quantum wells is explained as follows. The X_s^- , which at $B = 25$ T is the trion ground state in the absence of significant $e-h$ layer separation (i.e., in narrow or symmetric wells), is smaller and has different charge distribution than the X_t^- . This difference has little effect on Laughlin correlation with electrons, which avoid small relative $e-X^-$ pair angular momenta rather than approach closely to probe the X^- 's internal structure. However, it affects interactions with the QPs.

Indeed, the \mathcal{X}_s dispersion in Fig. 6(c) differs from \mathcal{X}_t of Fig. 3(c) and indicates stronger \mathcal{X}^- -QH attraction. We compare $\Delta^0 \sim 2$ meV with $\Delta_{LJ} = 2.02$ meV ($\mathcal{E}_{QE} = 1.38$ meV and $\mathcal{E}_{QH} = 0.64$ meV) using Eq. (1) to find that Δ^- is very small (to prevent distinction of the \mathcal{X} and \mathcal{X}^- emission peaks) or even negative.

Negative Δ^- , as in Fig. 6(b), means that the \mathcal{X}^- binds the first QH so strongly that even in the absence of free QHs it is unstable toward creation of a new QE-QH pair ($\mathcal{X}^- \rightarrow \mathcal{X} + \text{QE}$). And negative Δ^+ in Fig. 6(d) means that a second QH is not bound at all. As a result, the (neutral) \mathcal{X} is the most strongly bound state regardless of the presence of either QEs or QHs. This precludes discontinuity in PL at $\nu = 1/3$ in a 10 nm quantum well.

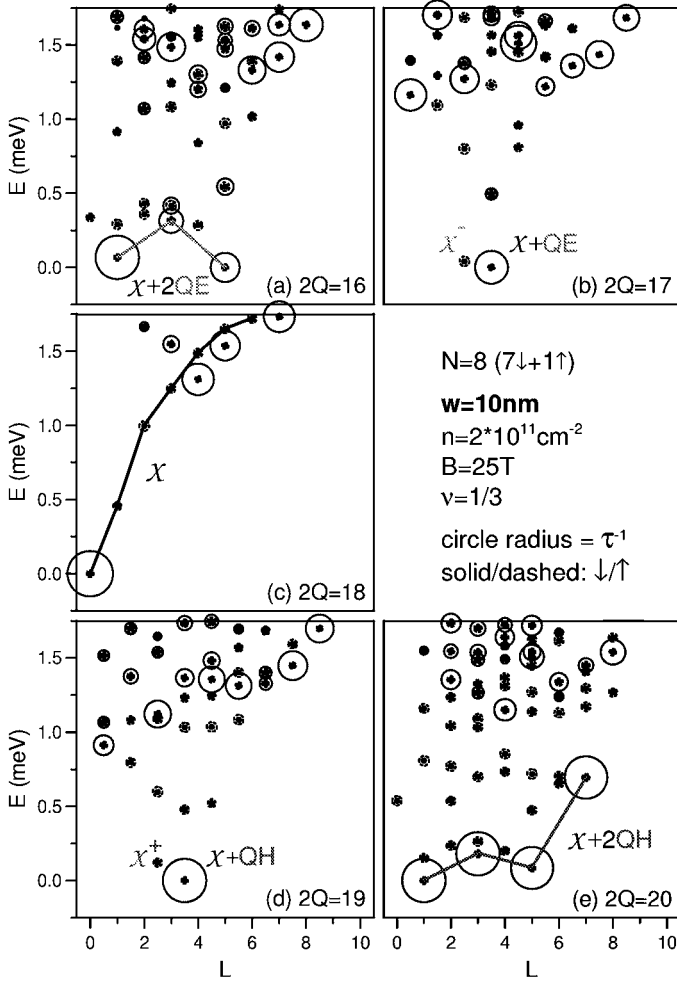


Fig. 6. Excitation spectra similar to Fig. 3, but calculated for $8e + h$ systems, with a modified $e-e$ pseudopotential (see text), with one reversed-spin electron, and for the well width $w = 10$ nm.

9. Wider Wells

For $n = 2 \cdot 10^{11} \text{ cm}^{-2}$ and $w \geq 40$ nm, the QXs are replaced by “anyon excitons” hQE_μ (proposed earlier in ideal bilayer systems¹⁵). Their recombination also causes a jump in PL energy at $\nu = 1/3$, but it can be easily distinguish from that due to QXs since it is much larger ($\sim \Delta_{LJ}$) and goes in the *opposite direction*.

10. Conclusion

We studied PL of incompressible electron liquids formed in a 2DEG in high magnetic fields. The emission spectrum is found due to the recombination of neutral and fractionally charged *quasiexcitons* (QXs). These novel bound state are formed

from trions by Laughlin correlation with the surrounding electrons. The energy and recombination spectrum of the QXs critically depends on the well width, electron concentration, and the magnetic field, offering explanation for the discontinuities observed in PL in coincidence with the fractional quantum Hall effect.

Acknowledgment

The authors gratefully acknowledge discussions with M. Byszewski, M. Potemski, and P. Hawrylak, and financial support from grants DE-FG 02-97ER45657 of US DOE and N20210431/0771 of the Polish MNiSW.

References

1. D. C. Tsui, H. L. Störmer, and A. C. Gossard, *Phys. Rev. Lett.* **48**, 1559 (1982).
2. R. B. Laughlin, *Phys. Rev. Lett.* **50**, 1395 (1983).
3. S. L. Sondhi, A. Karlhede, S. A. Kivelson, and E. H. Rezayi, *Phys. Rev. B* **47**, 16419 (1993).
4. D. Heiman, B. B. Goldberg, A. Pinczuk, C. W. Tu, A. C. Gossard, and J. H. English, *Phys. Rev. Lett.* **61**, 605 (1988).
5. B. B. Goldberg, D. Heiman, A. Pinczuk, L. N. Pfeiffer, and K. West, *Phys. Rev. Lett.* **65**, 641 (1990).
6. I. V. Kukushkin and V. B. Timofeev, *Adv. Phys.* **45**, 147 (1996).
7. C. Schüller, K.-B. Broocks, P. Schröter, Ch. Heyn, D. Heitmann, M. Bichler, W. Wegscheider, T. Chakraborty, and V. M. Apalkov, *Phys. Rev. Lett.* **91**, 116403 (2003).
8. M. Byszewski, B. Chwalisz, D. K. Maude, M. L. Sadowski, M. Potemski, T. Saku, Y. Hirayama, S. Studenikin, D. G. Austing, A. S. Sachrajda, and P. Hawrylak, *Nature Physics* (London) **2**, 239 (2006).
9. K. Kheng, R. T. Cox, Y. Merle d'Aubigne, F. Bassani, K. Saminadayar, and S. Tatarenko, *Phys. Rev. Lett.* **71**, 1752 (1993).
10. G. Yusa, H. Shtrikman, and I. Bar-Joseph, *Phys. Rev. Lett.* **87**, 216402 (2001).
11. A. Wójs, J. J. Quinn, and P. Hawrylak, *Phys. Rev. B* **62**, 4630 (2000).
12. I. V. Lerner and Yu. E. Lozovik, *Zh. Eksp. Teor. Fiz.* **80**, 1488 (1981).
13. A. H. MacDonald and E. H. Rezayi, *Phys. Rev. B* **42**, 3224 (1990).
14. X. M. Chen and J. J. Quinn, *Phys. Rev. Lett.* **70**, 2130 (1993).
15. A. Wójs and J. J. Quinn, *Phys. Rev. B* **63**, 045303 (2001); *ibid.* **63**, 045304 (2001).
16. F. D. M. Haldane, *Phys. Rev. Lett.* **51**, 605 (1983).
17. A. Wójs and J. J. Quinn, cond-mat/0609103.
18. I. H. Tan, G. L. Snider, L. D. Chang, and E. L. Hu, *J. Appl. Phys.* **68**, 4071 (1990).
19. A. Wójs and P. Hawrylak, *Phys. Rev. B* **51**, 10880 (1995).
20. F. D. M. Haldane, *The Quantum Hall Effect*, eds. R. E. Prange and S. M. Girvin (Springer-Verlag, New York, 1987), chapter 8, pp. 303–352.
21. A. Wójs, I. Szlufarska, K. S. Yi, and J. J. Quinn, *Phys. Rev. B* **60**, 11273 (1999).
22. J. K. Jain, *Phys. Rev. Lett.* **63**, 199 (1989).
23. E. H. Rezayi and F. D. M. Haldane, *Phys. Rev. B* **32**, 6924 (1985).